Available online at www.sciencedirect.com

ScienceDirect

Procedia Engineering 66 (2013) 723 – 736

Procedia Engineering

www.elsevier.com/locate/procedia

5th Fatigue Design Conference, Fatigue Design 2013

Fatigue damage modelling of continuous E-glass fibre/epoxy composite

Rim Ben Toumi [a,b], Jacques Renard [a], Martine Monin [b], Pongsak Nimdum [a]

[a]*Centre des Matériaux Pierre-Marie Fourt, Ecole des Mines de Paris, BP 87, 91003 Evry Cedex, France*

[b]*PSA Peugeot-Citroën, Centre technique La Garenne, 18 rue des Fauvelles, 92250 LA GARENNE-COLOMBES Cedex, France*

Abstract

Static and fatigue tension tests have been performed on continuous E-glass fibre reinforced epoxy composite.
All tests were followed by non-destructive techniques: acoustic emission records (AE) and microscopic observations in addition to stiffness monitoring with an extensometer in order to investigate damage mechanisms occurring under both static and fatigue loadings.
The data obtained were used to identify the modes of damage and its effects on the macroscopic behaviour of the composite material under both static and fatigue loading. Then, a fatigue model was used to predict the fatigue life of the composite under tension-tension cyclic tests. This model reduces drastically the number of fatigue tests required to obtain S-N curves.
Experimental data were in excellent agreement with model predictions.

Keywords: Fatigue life model; E-glass fibre/epoxy composite; Damage mechanisms; Acoustic emission

doi:10.1016/j.proeng.2013.12.126

1. Introduction

One of the most attractive candidates to composite materials is the automotive industry. As continuous fibre-reinforced composites provide good mechanical properties, they have been increasingly used in many lightweight structures such as structural automotive parts which were subjected in service to fatigue loadings. Therefore, a good prediction of fatigue life is required.

In this paper, a comparison between damage mechanisms and mechanical behavior under static and fatigue loadings will be done based on microscopic observations and acoustic emission records.
Then, a fatigue life model will be presented and applied to the studied composite material.
Unlike other fatigue life models requiring significant amount of experimental data, the semi-empirical model used in this work can predict the fatigue behavior using a well-defined minimum number of tests.
The effect of frequency and stress ratio are accounted for in this model.

Nomenclature

C_1, C_2, m_1, m, b, A, and B	material constants
n	number of cycles
N	number of cycles to failure
α, β	material constants
σ_u	ultimate stress of the virgin material
σ_{max}	maximum applied stress
R	stress ratio

2. Material and experimental methods

2.1 Material

In this work, an E-glass/epoxy woven fabric composite with a fibre volume fraction of 54% was studied. Mechanical properties of the material were obtained from mechanical characterization tests.
Specimens are cut into the epoxy resin based 2D glass fibre woven fabric manufactured by Resin Transfer Moulding (RTM) processing technology. Figure 1 shows the glass woven fabric without resin. The composite material consists of 10 layers. Each ply is a 2D glass fibre woven fabric: 97% of the glass woven fabric is in the warp direction (0°). While 3% are in the weft direction (90°).

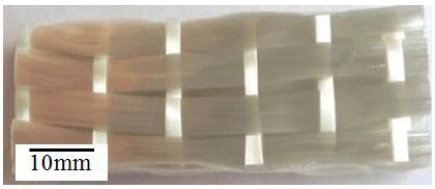

Fig.1. 2D glass fibre woven fabric

Material elastic properties were obtained from mechanical characterization tests: quasi-static tensile tests at 0°, 45° and 90°were performed in addition to short beam shear tests at both 0° and 90° directions. The table 1 summarizes the material properties.

Table 1. Mechanical properties of E-glass/epoxy composite

E1 *(MPa)*	*E2* *(MPa)*	*E3* *(MPa)*	*G12* *(MPa)*	*G23* *(MPa)*	*G13* *(MPa)*
40000	*16180*	*7000*	*2900*	*890*	*2200*

2.2 Experimental methods

A good understanding of damage mechanisms at each stress level is required to identify the chronology of damage modes occurring under quasi-static tests. Therefore static loading-unloading tests were carried out at a loading rate of 1MPa/s.
The test procedure is shown at figure 2.

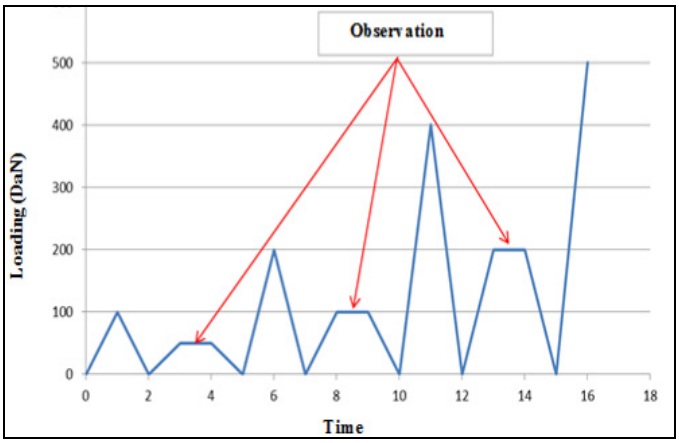

Fig.2. Quasi-static loading/unloading test procedure

Tensile-tensile fatigue experiments were performed at a frequency, f = 5Hz, with a stress ratio R=0.1, ($R= \sigma_{min}/\sigma_{max}$). Specimens 250 mm long by 25 mm wide with a thickness of 4 mm were cyclically tested with a servo-hydraulic testing machine. Also, acoustic emission records and microscopic observations after a certain number of cycles were used to understand fatigue damage mechanisms.

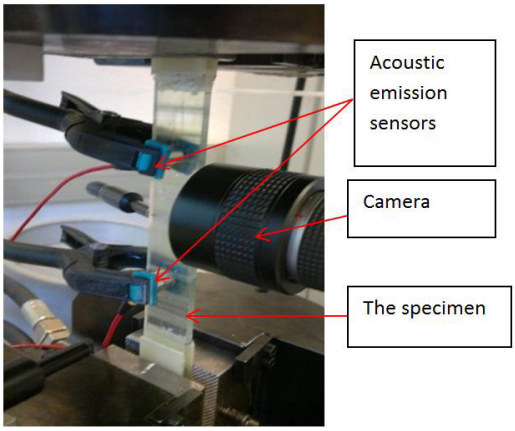

Fig.3.Experimental set-up

The problem encountered in achieving tensile-tensile fatigue tests at direction 0° was the specimen failure in the grips.
Figure 4 shows that highest temperature is localized at the tabs of the specimen. This information is an indication of stress concentration in these areas. Therefore, it was preferred to use thinner plates (2mm thick) in order to reduce the clamping stress.

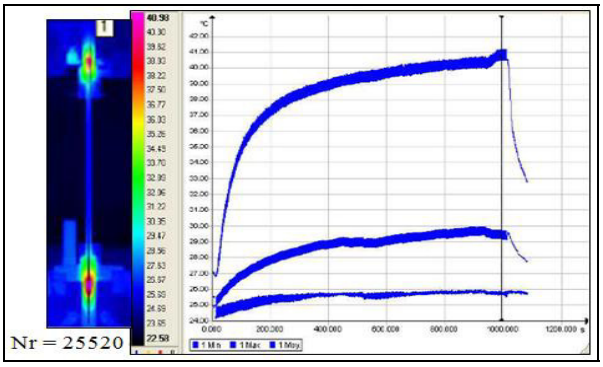

Fig.4. Temperature profile of a sample under fatigue loading

3. Results and discussion

3.1 Static and fatigue damage mechanisms

AE technique were used to detect cracks taking place during cycle evolution. Microscopic observations of specimen' polished edge at a given number of cycles provided accurate description of damage mechanisms evolution under static and fatigue loadings. For quasi-static loading-unloading tensile tests, microscopic observations were carried out during planned observation period.

Static damage mechanisms:

Figure 5 shows the damage mechanisms during longitudinal tensile tests: transverse microcracks at weft direction (90°): matrix cracking is accompanied by debonding at the fibre/matrix interface. Then, a longitudinal crack at the loading direction (0°) appeared just before the sample failure.

Main static damage modes observed at tensile directions 90° and 45° are: matrix cracking and fibre/matrix interface debonding. (Figures 6 and 7)

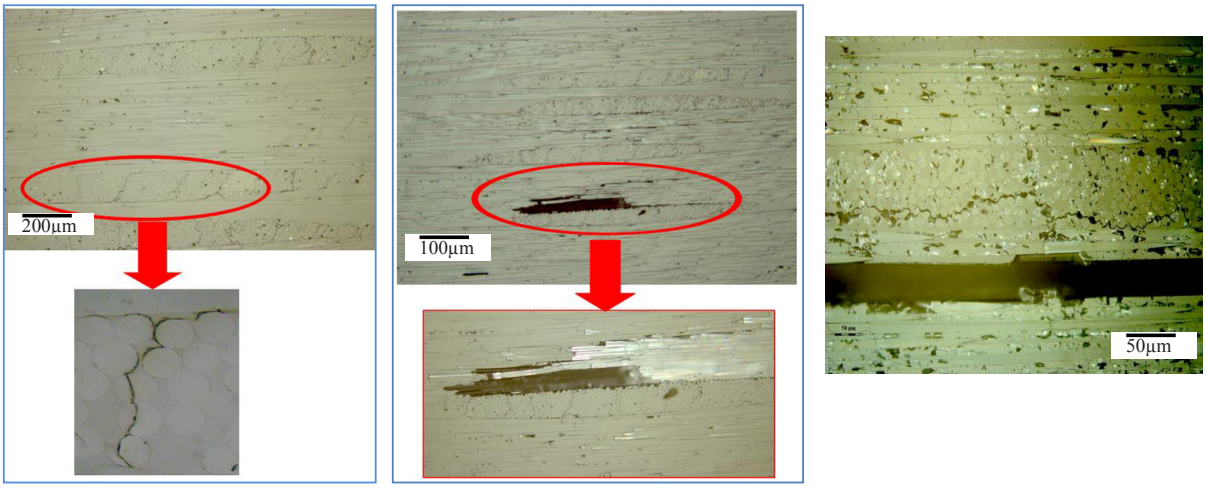

Fig.5. Damage mechanisms under quasi-static tensile test at direction 0°

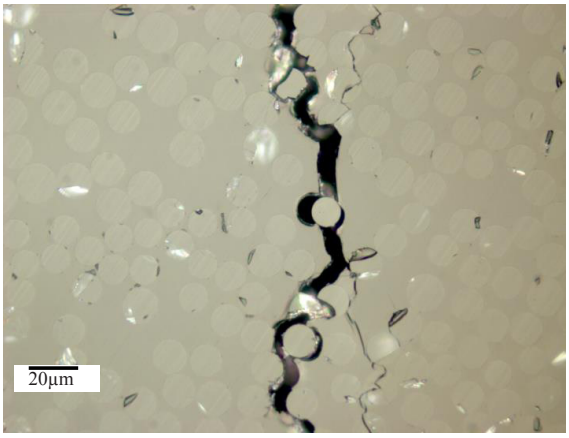

Fig.6. Damage mechanisms under quasi-static tensile test at direction 90°

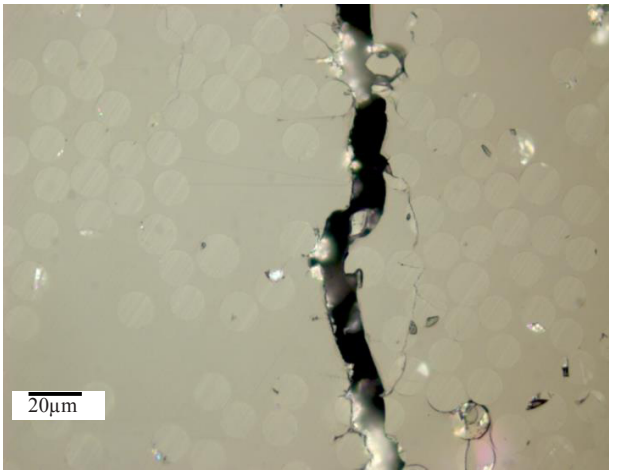

Fig.7. Damage mechanisms under quasi-static tensile test at direction 45°

Fatigue damage includes mainly these failure modes: transverse matrix cracking, delamination, splitting and fibre breakage. At figure 8, it can be seen some of these damage modes such as fibre/matrix interface debonding and fibre breakage at direction 0°.

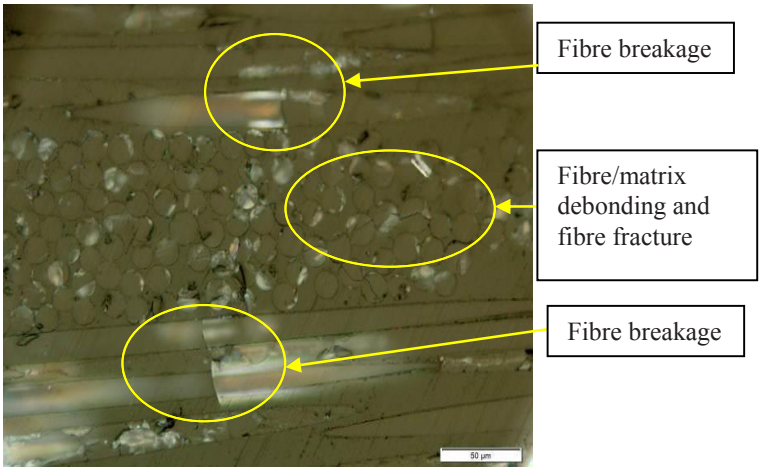

Fig.8. Microscopic observation of damage modes under fatigue loading

Acoustic emission records

- Tensile tests at direction 0°

Acoustic emission events have been recorded during static tensile tests and static loading-unloading tensile tests.

Two damage modes were identified:

Figures 9 and 10 show, respectively, the cumulative acoustic emission event count and cumulative acoustic emission

energy. These curves have two slopes significantly different.

The first damage onset is detected at the beginning of the test (at 200 MPa stress), when a low energy level is reached with a low acoustic events number. Based on microscopic observations, the corresponding stress level can be attributed to initiation of new transverse microcracks in the weakest locations.
Up to this level stress, the number of transverse cracks, formed by matrix cracking and fibre/matrix interface debonding, increases rapidly up to saturation density.
By the end of the test (up to 700 MPa), a second damage mode was detected by an increase in the slope of the number of events, both the energy content and event count rise quickly, and the specimen starts to emit popping sounds indicating extensive appearance of relatively larger transverse and longitudinal cracks.

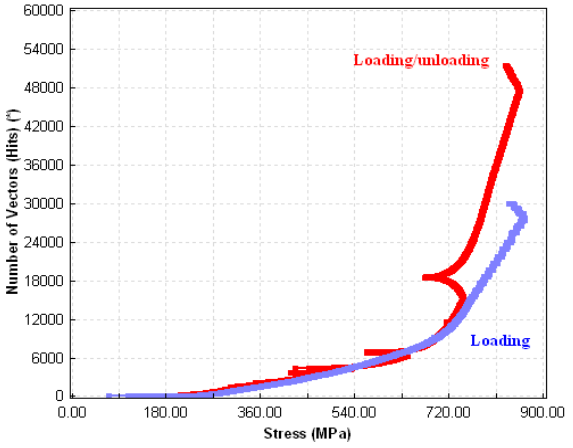

Fig.9. Evolution of the number of events with stress level

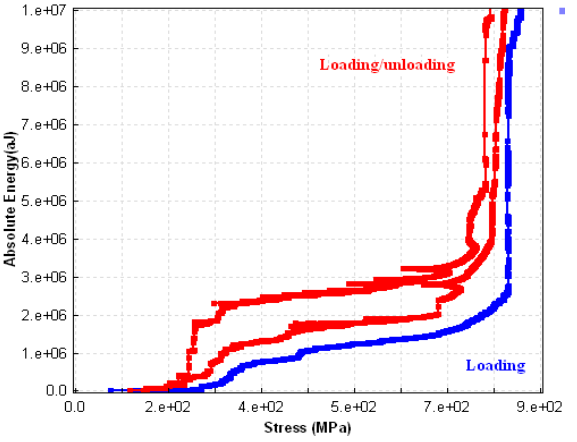

Fig.10. Evolution of the absolute energy with stress level

- Tensile-tensile fatigue tests at direction 0°

Figure 11 shows acoustic emissions records during tensile-tensile fatigue test at direction 0°. The greater number of events occurred at the first cycle. A saturation level of transverse cracks was reached. The second damage mode (longitudinal cracks) was developed during cyclic evolution leading to the sample failure.

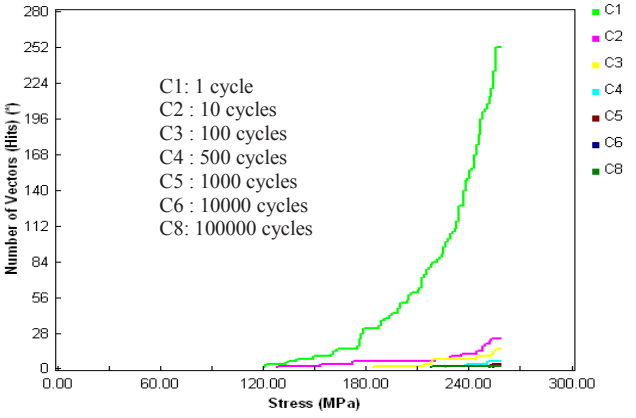

Fig.11. Evolution of the number of events with stress level for tensile tensile-tensile fatigue test at direction 0°

- *Stiffness evolution*

Both stress range and strain (at the loading direction) have been recorded during all tests.

Figures 12-14 inclusive show the evolution of the stiffness at directions 0°, 90°and 45° of quasi-static tensile tests.

Stiffness at both longitudinal and transverse directions is not affected until the final failure of the sample. For shear tensile test at 45°, a decrease of the stiffness was observed by the end of the test.

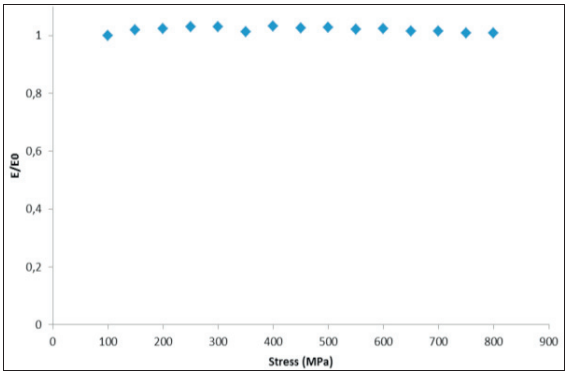

Fig.12. Evolution of the stiffness with stress level for quasi-static longitudinal tensile test (0°)

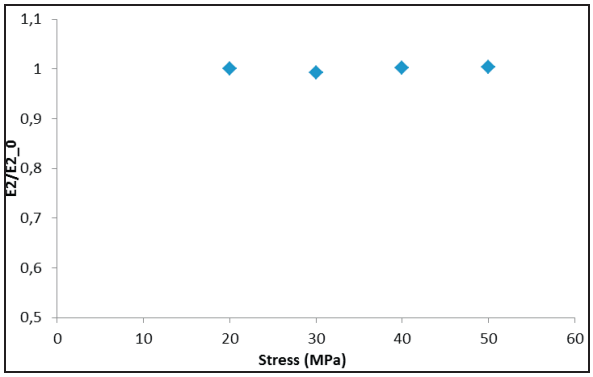

Fig.13. Evolution of the stiffness with stress level quasi-static transverse tensile test (90°)

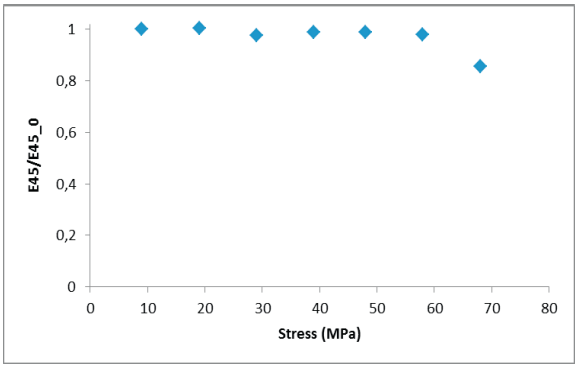

Fig.14. Evolution of the stiffness with stress level for quasi-static tensile test at direction 45°

The evolution of stiffness with stress level under cyclic loadings at the directions: 0°, 90° and 45° is shown by figures 15 to 17.

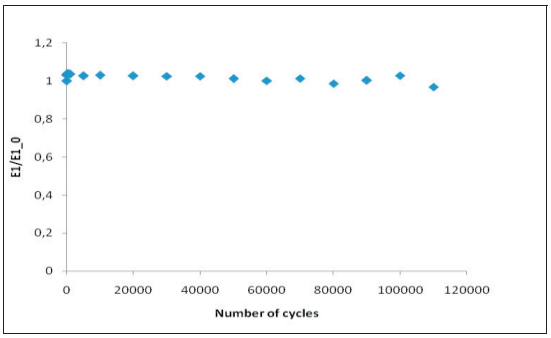

Fig.15. Evolution of the stiffness with stress level for tensile-tensile test at longitudinal direction (0°)

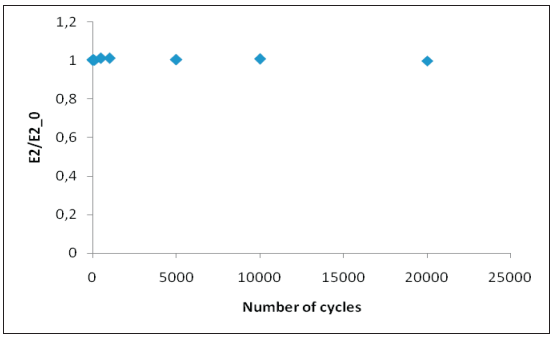

Fig.16. Evolution of the stiffness with stress level tensile-tensile test at transverse direction (90°)

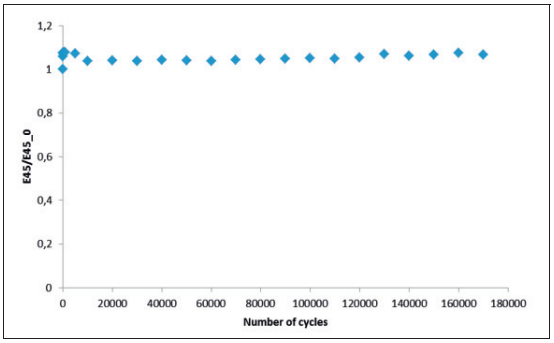

Fig.17. Evolution of the stiffness with stress level for tensile-tensile test at direction 45°

These curves indicate no loss of stiffness until the sudden failure of the specimens despite of observed under both static and fatigue loadings.

3.2 Fatigue model

Phenomenological approaches to modelling fatigue failure are mostly stiffness-based or strength-based. More exhaustive reviews are provided by Sendeckyj [1], Degrieck and Van Paepegem [2]. These approaches can be deterministic or probabilistic [3].
Two types of equations are generally used to model fatigue data, logarithmic:

$$S(N) = m.\log(N) + b \quad (1)$$

And power law:

$$S(N) = A.N^{B} \quad (2)$$

With S is the maximum applied stress and N is the number of cycles to failure and m, b, A, and B are constants.

Logarithmic models have been largely used as they generally fit all data, including static data, fairly well.
Power law models tend to provide improved fit at high cycles [4] [5]. As the objective of this work is to design structural parts under high number of cycles, a power law model will be used.

In this work, a fatigue life model based on S-N curves is used to predict the number of cycles to failure occurring under fixed loading conditions. Damages accumulation is not taken into account.

Sendeckyj [6] suggested that the residual strength after constant amplitude fatigue cycles is related to the initial initial ultimate static strength by a deterministic equation. The starting point of the model is this equation proposed by Caprino and D'Amore [2] [7]:

$$\frac{d\sigma}{dn} = -C_1 n^{-m_1} \tag{3}$$

As the model is for constant frequency loading, there is a simple link between cycle and time domains:

$$\frac{d\sigma}{dt} = -C_2 t^{-m_1} \tag{4}$$

Where n is the number of fatigue cycles, σ is the residual strength after n cycles, m_1 is a material constant and $C_2 = A.F(R,\sigma_u,\sigma_{\max})$, A is a constant, σ_u is the initial residual strength, σ_{max} is the maximum applied stress and R is the stress ratio.

Fatigue failure occurs when σ_u decreases to be equal to σ_{max}. The number of cycles required to degrade the material strength from σ_u to σ_{max} is the fatigue life of the material.

Based on the deterministic equations developed by Sendeckyj [6] and Herzberg and Manson [8] and recalled by Epaarachchi and Clausen [7], the following equations are obtained:

$$F(R,\sigma_u,\sigma_{\max}) = \sigma_u^{1-\gamma}\sigma_{\max}^{\gamma}(1-R)^{\gamma} \quad \text{for tension-tension and reverse loading.} \tag{5}$$

$$F(R,\sigma_u,\sigma_{\max}) = \sigma_u^{1-\gamma}\sigma_{\max}^{\gamma}(1-\frac{1}{R})^{\gamma} \quad \text{for compression-compression loading.} \tag{6}$$

Where $\gamma = 1.6 - \sin\theta$ (7)

θ is the smallest angle between the fibre direction and the load direction.

By integrating the equation (4) from t= t_0, the first static cycle, to t=T, the time when the failure occurs:

$$\left(\sigma_{\max} - \sigma_u\right) = -\frac{C_2}{-m_1+1} t^{-m_1+1}\Big|_{t=t_0,n=1}^{t=T,n=N} \tag{8}$$

Where $t = \frac{n}{f}$

By substituting C_2 for equation (5):

$$\left(\sigma_{\max}-\sigma_u\right)=-\frac{AF(R,\sigma_u,\sigma_{\max})}{-m_1+1}\frac{1}{f^{-m_1+1}}(N^{-m_1+1}-1) \tag{9}$$

For simplicity we consider:

$$\alpha=-\frac{A}{-m_1+1} \tag{10}$$

$$\beta=-m_1+1 \tag{11}$$

Here only tension-tension tests were performed.

The model can be written as:

$$\left(\frac{\sigma_u}{\sigma_{\max}}-1\right)\left(\frac{\sigma_u}{\sigma_{\max}}\right)^{\gamma-1}\frac{1}{(1-R)^{\gamma}}f^{\beta}=\alpha(N^{\beta}-1) \tag{12}$$

Or

$$\left(\frac{\sigma_u}{\sigma_{\max}}-1\right)\left(\frac{\sigma_u}{\sigma_{\max}}\right)^{\gamma-1}\frac{1}{(1-R)^{\gamma}}=\alpha(N^{\beta}-1)f^{-\beta} \tag{13}$$

This model has only two parameters to be determined α and β from experimental data.
A trial-and-error method was used to determine appropriate values of α and β. For each experimental data set
The left-hand side of the equation (13) was plotted against the quantity $(N^{\beta}-1)f^{-\beta}$ for a trial value of β.
This procedure is repeated until the best-fit straight line passes through the origin.
α is given by the slope of the linear regression straight line.

It is recommended to calculate α and β using data sets from tests performed at a stress ratio R=0.1 for tension-tension and R=10 for compression-compression in order to minimize the errors caused by the scatter in the fatigue data set [6] [7].

Figure 18 shows the procedure used to calculate the appropriate values of α and β for the loading direction 45°.

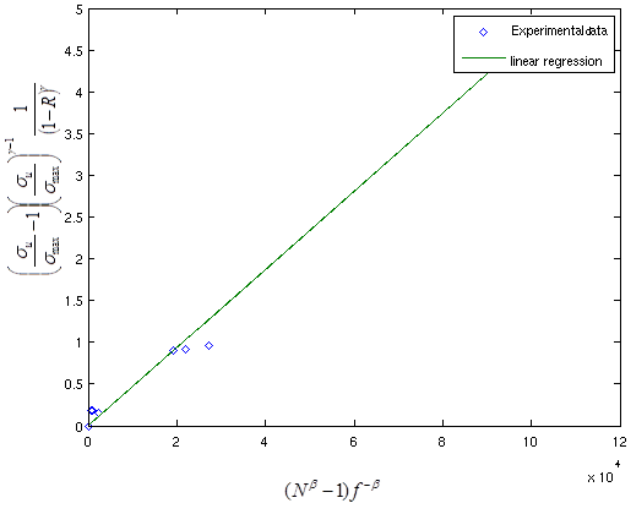

Fig.18. $(N^{\beta}-1)f^{-\beta}$ *plot and fitted line for tensile-tensile at the loading direction 45°*

This procedure is applied to calculate α and β for each loading direction 0° and 90°.
Figures 19-21 inclusive show the calculated and experimental curves for tension-tension fatigue tests at directions: 0°, 90° and 45°.
The proposed model is in good agreement with the available experimental data.

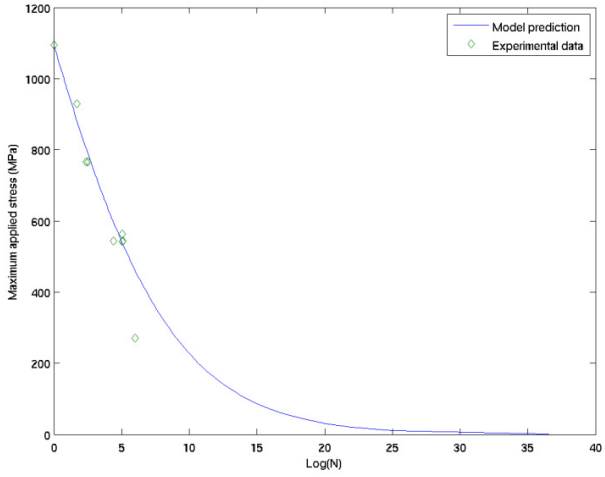

Fig.19. Fatigue behaviour under tension-tension loading at direction 0°

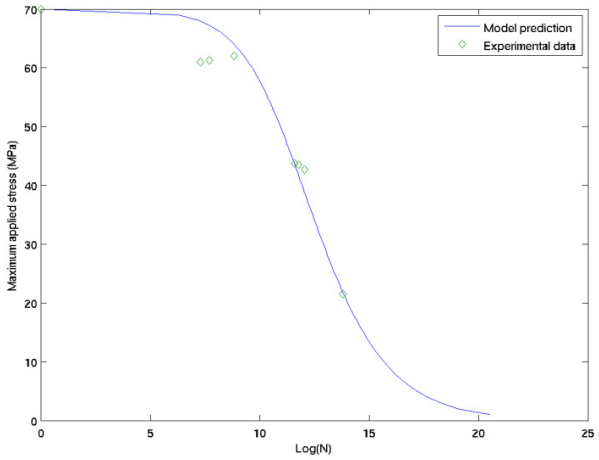

Fig.20. Fatigue behaviour under tension-tension loading at direction 90°

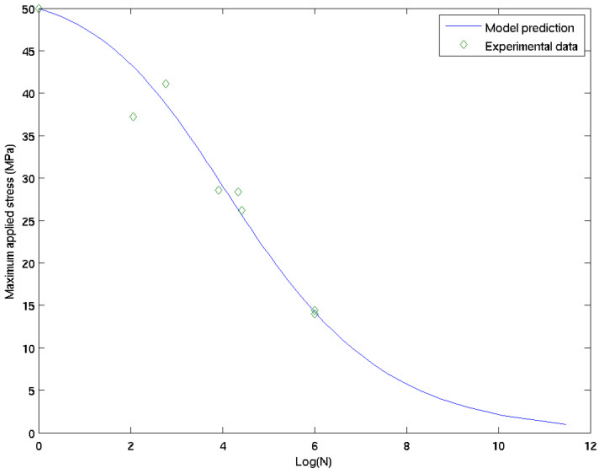

Fig.21. Fatigue behaviour under tension-tension loading at direction 45°

4. Conclusions

Based on microscopic observations and acoustic emission records under both static and cyclic loadings, the composite behaviour was investigated under static and fatigue loadings. It was found that failure modes under fatigue loading are the same as static damages. In addition to this, there is no stiffness loss for static and fatigue case.

A semi-empirical fatigue model for life prediction including the effects of stress ratio, frequency and maximum stress was used. The model followed is based on the assumption of a strength degradation of the composite material according to a power law.

The fatigue model predictions were found to be in good agreement with experimental data for tension-tension fatigue behaviour.

Future work will be focused on studying the fatigue behaviour from a statistical point of view in order to take into account the scatter generally affecting fatigue tests.

Acknowledgements

The authors would like to thank HUTCHINSON company for providing the composite material used in this work.

References

[1] Sendeckyj, G.P, '*Life Prediction for Resin-Matrix Composite Materials'*. Composite Materials Series: Fatigue of composites, K.L, Reifsnider, ed., New York: Elsevier Science Publishers, 4:431-483, 1990.

[2] Degriech. J and Van Paepegem.W, '*Fatigue Damage Modelling of fibre-reinforced composite materials'*. Applied Mechanics Reviews, *54. (4)* 279-300, 2001.

[3] Qiao, P. and Yang,.M., '*Fatigue Life Prediction of Pultruded E-Glass/Plyurethane Composites*'. Journal of composite materials, Vol.40, N0.9/2006.

[4] Mandell, J.F., Samborsky, D.D., and Cairns, D.S. '*Fatigue of Composite Materials and Substructures for Wind Turbine Blades'*, Contractor Report SAND2002-0771, Sandia National Laboratories, Albuquerque, NM (2002).

[5] Whitney, J.M., '*Fatigue Characterization of Composite Materials*', ASTM STP 723, American Society for Testing and Materials, 1981.

[6] Sendeckyj, G.P., '*Fitting Models to Composite Materials Fatigue Data*', ASTM STP 734, American Society for Testing and Materials, 1981.

[7] Epaarachchi, J.A, Clausen P.D., '*An empirical model for fatigue behavior prediction of glass fibre-reinforced plastic composites for various stress ratios and test frequencies'*. Composites: Part A 34 (2003) 313-326.

[8] Hertzberg RW, Manson JA, *Fatigue of engineering plastics*; New York: Academic Press;